



# Magnetically recyclable Ru immobilized on amine-functionalized magnetite nanoparticles and its high selectivity to prepare *cis*-pinane

Yue Liu<sup>a</sup>, Lu Li<sup>b</sup>, Shiwei Liu<sup>b</sup>, Congxia Xie<sup>a</sup>, Shitao Yu<sup>b,\*</sup>

<sup>a</sup> Key Laboratory of Sensor Analysis of Tumor Marker Ministry of Education, College of Chemistry and Molecular Engineering, Qingdao University of Science and Technology, 53 Zhengzhou Road, Qingdao 266042, People's Republic of China

<sup>b</sup> College of Chemical Engineering, Qingdao University of Science and Technology, 53 Zhengzhou Road, Qingdao 266042, People's Republic of China



## ARTICLE INFO

### Article history:

Received 6 July 2016

Received in revised form 30 August 2016

Accepted 4 September 2016

Available online 7 September 2016

### Keywords:

Fe<sub>3</sub>O<sub>4</sub>/1, 6-hexanediamine/Ru

Magnetic separation

α-Pinene

Hydrogenation

## ABSTRACT

*cis*-Pinane was efficient and selective prepared through the hydrogenation of α-pinene base on Ru nanoparticles stabilized by amine-functionalized magnetite nanoparticles (Fe<sub>3</sub>O<sub>4</sub>/NH<sub>2</sub>/Ru). The effects of changing carbon chain length on amine-functionalized catalyst formation have also been investigated. The characterization results showed that Ru nanoparticles could be efficient loaded by 1, 6-hexanediamine functionalized magnetite nanoparticles. At the same time, Fe<sub>3</sub>O<sub>4</sub>/1, 6-hexanediamine/Ru had good superparamagnetic properties and that the introduction of the amine-functionalized improved the monodispersity, morphological regularity and size uniformity of the Ru nanoparticles. The Fe<sub>3</sub>O<sub>4</sub>/1, 6-hexanediamine/Ru catalyst was completely recoverable with the simple application of an external magnetic field and the catalytic efficiency showed no obvious loss for the hydrogenation of α-pinene even after ten repeated cycles.

© 2016 Elsevier B.V. All rights reserved.

## 1. Introduction

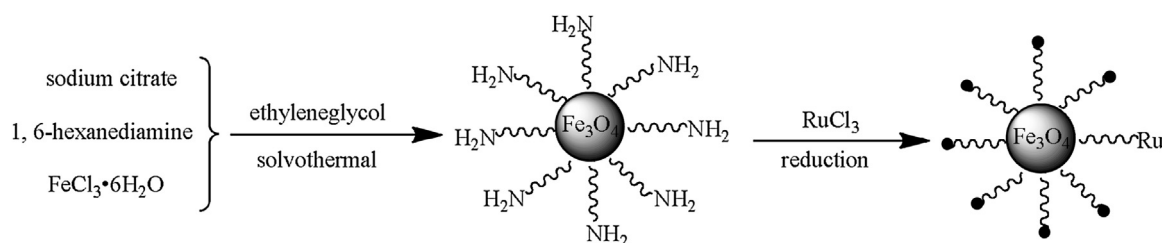
*cis*-Pinane is a distinctly important industrial intermediate and widely used for the synthesis of specialty chemicals and pharmaceuticals such as dihydromyrcenol, linalool and other terpene series species [1]. Conventionally, *cis*-pinane is industrially prepared through the hydrogenation of α-pinene in the presence of some noble metal catalysts, such as Pd/C or Pt/C [2,3]; however, both catalysts show a low selectivity towards *cis*-pinane. The identification of highly active and selective catalysts is a crucial aspect for the efficiency of the process. Ru-based catalysts have been found to exhibit good catalytic performance towards hydrogenation of compounds such as levulinic acid [4], phenol [5], aldimines [6] and γ-valerolactone [7]. Ru-based catalysts are also used in the hydrogenation of α-pinene. RuCl<sub>3</sub> dissolved in water showed good catalytic properties, with 99.7% conversion of α-pinene and 96.3% selectivity towards *cis*-pinane [8]. The main drawback observed in the use of this catalyst was its deactivation over time due to the agglomeration of Ru nanoparticles originating from the hydrogenation of RuCl<sub>3</sub>. The use of Ru nanoparticles protected by poly(ethylene oxide)-*b*-poly(propylene oxide)-*b*-poly(ethylene oxide) triblock copolymer P123 (PEO<sub>20</sub>-PPO<sub>70</sub>-PEO<sub>20</sub>, average

molecular weight 5800) micelles distinct improved the molar ratio between *cis*-pinane and *tran*-pinane produced from the hydrogenation of α-pinene [9]; however, as a non-ionic surfactant, stabilizer P123 brought to the production of an emulsion, consisting in the oil-soluble product and the water containing the Ru. As a result, it was difficult to separate the product from the emulsified mixture. Although an extraction method could be used to separate the product from the emulsion system, the use of an extracting agent could destroy the stability of the nanoparticles. These considerations indicate the importance of developing an inert support to stabilize Ru nanoparticles and to find a convenient separation method for the products of the α-pinene hydrogenation reaction.

Recently, immobilizing noble metal nanocatalysts on Fe<sub>3</sub>O<sub>4</sub> magnetic support have been widely used due to their good separation performance in the presence of an appropriate magnetic field [10–18]. Pure Fe<sub>3</sub>O<sub>4</sub> particles, lacking functional groups on their surface, hardly adsorb any metal nanoparticles [19]. Considering the above limitations, coating materials such as silica, polymers, and carbon should therefore be used as shells, to add the necessary functional groups to the Fe<sub>3</sub>O<sub>4</sub> spheres [20–22]. However, a drawback is that the coating materials need further chemical functionalization, and the process is relatively complicated. Therefore, developing a simple and facile approach to modify magnetic nanoparticles is highly desirable. Very recently, much attention has been focused on amine functionalization, since amines are well known to stabilize nanoparticles against aggregation without dis-

\* Corresponding author.

E-mail address: [yushitaoqust@126.com](mailto:yushitaoqust@126.com) (S. Yu).



**Scheme 1.** Synthesis route of  $\text{Fe}_3\text{O}_4$ /1, 6-hexanediamine/Ru magnetite nanoparticles.

turbing their desirable properties [23–25]. The synthesis process was simple and facile to obtain amine-functionalized magnetic nanoparticles, allowing an easy loading of noble metal nanoparticles on its surface. At the same time, amine-functionalized magnetic nanoparticles catalysts have been found to show the high catalytic activity towards hydrogenation [26,27], Heck reaction [28,29], Suzuki reaction [30,31] and so on. In the present work,  $\text{Fe}_3\text{O}_4$ /1, 6-hexanediamine/Ru nanoparticles were successfully prepared using 1, 6-hexanediamine as the functional materials in the hydrothermal treatment. The catalyst obtained in this way was used in the hydrogenation of  $\alpha$ -pinene.

## 2. Experimental

### 2.1. Materials

The chemicals used in the course of the work were:  $\alpha$ -pinene,  $\text{RuCl}_3$ ,  $\text{PdCl}_2$ ,  $\text{FeCl}_3 \cdot 6\text{H}_2\text{O}$ , anhydrous sodium acetate, ethylene glycol, sodium citrate, ethanol, 1, 2-ethylenediamine, 1, 4-butanediamine, 1, 6-hexanediamine, 1, 8-octanediamine and 1, 12-dodecanediamine are of analytical grade and purchased from Shanghai Chemical Corp. Hydrogen (99.99 wt%) were obtained from Qingdao Airichem Specialty Gases & Chemicals Co. Ltd. All of these materials were commercially available and were used without further purification. Deionized water was used for all experiments.

### 2.2. Synthesis of $\text{Fe}_3\text{O}_4\text{-NH}_2\text{-Ru}$ magnetite nanoparticles

The preparation of  $\text{Fe}_3\text{O}_4$ /1, 6-hexanediamine/Ru was carried out in two steps, as shown in Scheme 1. To begin, the amine-functionalized magnetite particles were prepared by a versatile solvothermal reaction. 1.0 g of  $\text{FeCl}_3 \cdot 6\text{H}_2\text{O}$ , 2.0 g of anhydrous sodium acetate and 6.5 g 1, 6-hexanediamine were accurately mixed with 30 mL of ethylene glycol at room temperature for 2 h, using a mechanical stirring system. The homogeneous mixture was transferred to a 50 mL Teflon-lined stainless-steel autoclave and the reaction was carried out at 200 °C for 8 h. The reacted mixture was separated by applying an external magnetic field. The obtained magnetite particles were washed three times with water and dried at 60 °C for 4 h under a 500 Pa pressure, obtaining  $\text{Fe}_3\text{O}_4$ /1, 6-hexanediamine particles [23].  $\text{Fe}_3\text{O}_4$ /1, 2-ethylenediamine,  $\text{Fe}_3\text{O}_4$ /1, 4-butanediamine,  $\text{Fe}_3\text{O}_4$ /1, 8-octanediamine and  $\text{Fe}_3\text{O}_4$ /1, 12-dodecanediamine particles were prepared using a similar method.

In the second and final step, Ru nanoparticles were loaded onto the  $\text{Fe}_3\text{O}_4$ /1, 6-hexanediamine particles, using  $\text{RuCl}_3$  as the precursor. 0.2 g of  $\text{Fe}_3\text{O}_4$ /1, 6-hexanediamine, 0.1 g of  $\text{RuCl}_3$  and 50 mL of ethanol were dispersed for 40 min in an ultrasonic oscillator. Following the dispersion, 50 mL of 0.13 mol/L  $\text{NaBH}_4$  solution used as reducing agent were dropped into the mixture, which reacted at room temperature for 4 h.  $\text{Fe}_3\text{O}_4$ /1, 6-hexanediamine/Ru was separated by applying an external magnetic field, washing five times with water and drying at 60 °C for 4 h under 500 Pa

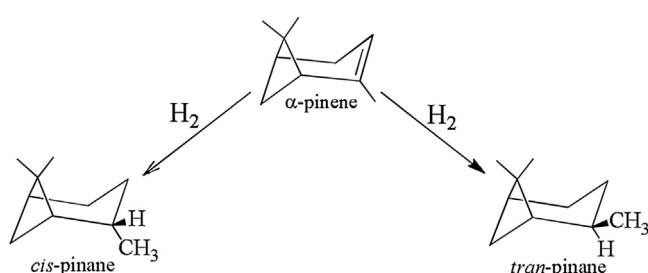
pressure [32]. The  $\text{Fe}_3\text{O}_4$ /1, 6-hexanediamine/Ru particles were analyzed by inductively coupled plasma-atomic emission spectrometry (ICP-AES) to determine the content of Ru nanoparticles.  $\text{Fe}_3\text{O}_4$ /1, 6-hexanediamine/Pd,  $\text{Fe}_3\text{O}_4$ /1, 6-hexanediamine/Rh and  $\text{Fe}_3\text{O}_4$ /1, 6-hexanediamine/Pt particles were prepared using a similar method.

### 2.3. Characterizations

Some samples of the intermediates and end-products were characterized using transmission electron microscopy (TEM), X-ray diffraction (XRD), Fourier transform infrared spectroscopy (FT-IR), ICP-AES, X-Ray photoelectron spectroscopy (XPS) and quantum design vibrating sample magnetometer. TEM analyses were carried out using a JEOL-1200 microscope, operated at 100 kV. FT-IR spectra were recorded in the wavelength range of 4500–400  $\text{cm}^{-1}$  on a Nicolet 510P FT-IR spectrometer using the KBr method. XRD patterns were collected on a Rigaku D/max-2400 diffractometer with Cu-K $\alpha$  anode radiation at 40 kV and 100 mA in the 2 $\theta$  range of 10–90° with a scan speed of 2°/min. XPS was carried out on a PHI-5702 instrument (Thermo Fisher Scientific-U. K; X-ray source: monochromated Al Ka,  $h\nu = 1486.6$  eV; X-ray energy: 15 kV, 150 W; Binding energies: C<sub>1s</sub> hydrocarbon peak at 284.60 eV). ICP-AES was performed using a Varian Vista Pro ICP-AES instrument running at 1200 W forward power. Before analysis, the samples were digested in a mixture of HF, HCl and  $\text{HNO}_3$ . Magnetic measurements were collected on a vibrating sample magnetometer at room temperature in an applied magnetic field sweeping from –15 to 15 kOe.

### 2.4. Catalytic reaction

The formula on hydrogenation of  $\alpha$ -pinene is shown in Scheme 2. Mixtures of different amounts of  $\alpha$ -pinene and catalyst was reacted at 160 °C for 5 h under 5 MPa  $\text{H}_2$  partial pressure in a 100 mL stainless steel reactor with mechanical stirring. After the reaction was completed, the catalyst was separated from the product phase by applying an external magnet. The product phase was analyzed using gas chromatography(GC) to determine the obtained conversion of  $\alpha$ -pinene and the selectivity towards cis-pinane. The catalyst layer was reused directly in the recycle experiments to



**Scheme 2.** The formula on hydrogenation of  $\alpha$ -pinene.

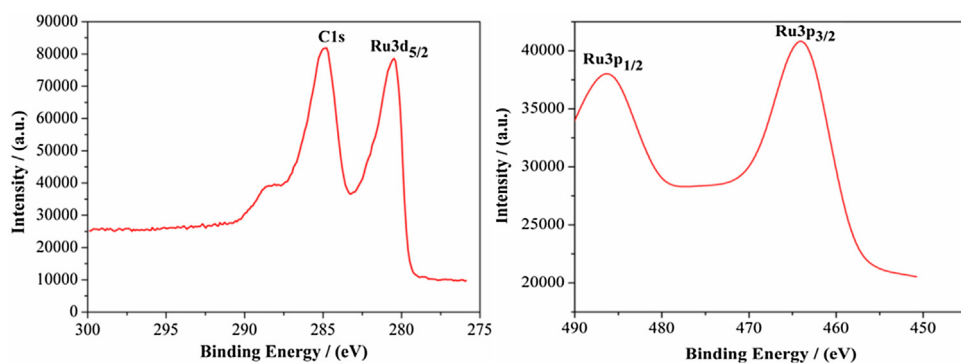


**Fig. 1.** XPS spectrum of the  $\text{Fe}_3\text{O}_4/1,6$ -hexanediamine/Ru.

examine its reusability. All experiments were repeated five times in order to determine the reproducibility of the results.

Samples of the products layer were characterized qualitatively using a gas chromatography-mass spectrometer (GC-MS) on an HP6890/5973 GC-MS equipped with an AT-5 capillary column ( $30\text{ m} \times 0.25\text{ mm} \times 0.25\text{ }\mu\text{m}$ ). Quantitative analyses were carried out using GC on an HP6890 GC equipped with a flame ionization detectoran (FID) and an AT-5 capillary column ( $30\text{ m} \times 0.25\text{ mm} \times 0.25\text{ }\mu\text{m}$ ). The temperatures of the injector and the detector were  $250^\circ\text{C}$  and  $260^\circ\text{C}$ , respectively. The temperature program was as follows: holding at  $80^\circ\text{C}$  for 2 min, increasing to  $180^\circ\text{C}$  at a rate of  $4^\circ\text{C}/\text{min}$  and finally holding at  $180^\circ\text{C}$  for 2 min. The qualitative analysis was conducted on the basis of the holding time of the peak. The content of reactants and products was directly obtainable by the GC chemstation system, according to the area of each chromatograph peak. The  $\alpha$ -pinene conversion was determined as a function of the mass of  $\alpha$ -pinene consumed in the reaction. The product selectivity was calculated by  $W_s/W_{\text{ALL}} \times 100$ , where  $W_s$  is the amount of the product for which selectivity is being evaluated and  $W_{\text{ALL}}$  is the total amount of the products, including *cis*-pinane and *trans*-pinane.

### 3. Results and discussion

#### 3.1. Effects of catalysts on reaction results

The work started with the screening of catalysts. Pd/C and Ru/C demonstrated the best performance towards the hydrogenation of the carbon-carbon double bond and were therefore used as the standard against which the behavior of all the other catalysts was compared [33,34]. The reaction results for the different catalysts are given in Table 1. It was seen that when no cata-

lyst was used, the hydrogenation reaction did not take place at all (Entry 1). The Pd/C and PdCl<sub>2</sub> showed poor catalytic performance, with both  $\alpha$ -pinene conversion and *cis*-pinane selectivity below 85% (Entries 2 and 3). Ru/C and RuCl<sub>3</sub> showed excellent catalytic properties towards hydrogenation. The  $\alpha$ -pinene conversion and *cis*-pinane selectivity were over than 95% and 94%, respectively (Entries 4 and 5). The above results indicate that Ru-based catalysts display a higher catalytic activity than the Pd-based catalyst; however, the reusability of RuCl<sub>3</sub> was poor (Fig. S1) due to the aggregation of the Ru nanoparticles which occurred after each cycle (Fig. S2) [35] and to the difficulty of separating the product from the product. Among all the  $\text{Fe}_3\text{O}_4$  supported catalysts, the non-functionalized magnetite nanoparticles Pd/ $\text{Fe}_3\text{O}_4$  and Ru/ $\text{Fe}_3\text{O}_4$  catalysts showed the poorest catalytic performance (Entries 7 and 8). This was due to the fact that the pure  $\text{Fe}_3\text{O}_4$  spheres had no functional groups on their surface hindering adsorption of the metal active center [19]. The amine-functionalized catalysts showed the best catalytic performance for hydrogenation (Entries 9–12). In particular,  $\text{Fe}_3\text{O}_4/1,6$ -hexanediamine/Ru showed an excellent catalytic activity towards hydrogenation: the  $\alpha$ -pinene conversion reached 99.2% and the *cis*-pinane selectivity was 97.1% (Entry 9). In order to explain the good catalytic performance of  $\text{Fe}_3\text{O}_4/1,6$ -hexanediamine/Ru, FT-IR spectra, XPS and TEM analyses were carried out. The results are shown in Figs. S3, 1 and 2. As shown in Fig. 1, the peaks present at 280.1 eV (assigned to Ru 3d<sub>5/2</sub>), 461.3 eV (assigned to Ru 3p<sub>3/2</sub>), and 484.4 eV (assigned to Ru 3p<sub>1/2</sub>) suggested the presence of Ru(0) in its elementary state [36]. In addition,  $\text{Fe}_3\text{O}_4/1,6$ -hexanediamine contains numerous amines groups (Fig. S3) and these functional groups served as anchors to immobilize Ru nanoparticles and facilitate their dispersion by preventing them from aggregating in solution [37]. From the TEM observations (Fig. 2b), numerous monodispersed

**Table 1**  
Effect of catalysts on the hydrogenation results.<sup>a</sup>

Entry	Catalyst	C/%	S/%
1	No catalyst	$1.2 \pm 0.1$	$69.3 \pm 0.2$
2	Pd/C	$83.6 \pm 0.2$	$78.1 \pm 0.5$
3	PdCl <sub>2</sub>	$85.0 \pm 0.3$	$80.2 \pm 0.3$
4	Ru/C	$95.8 \pm 0.3$	$94.9 \pm 0.1$
5	RuCl <sub>3</sub>	$97.9 \pm 0.2$	$95.8 \pm 0.3$
6 <sup>b</sup>	RuCl <sub>3</sub>	$81.2 \pm 0.3$	$95.1 \pm 0.2$
7	$\text{Fe}_3\text{O}_4/\text{Pd}$	$43.5 \pm 0.1$	$79.6 \pm 0.2$
8	$\text{Fe}_3\text{O}_4/\text{Ru}$	$49.7 \pm 0.5$	$95.3 \pm 0.4$
9	$\text{Fe}_3\text{O}_4/1,6$ -hexanediamine/Ru	$99.2 \pm 0.3$	$97.1 \pm 0.2$
10	$\text{Fe}_3\text{O}_4/1,6$ -hexanediamine/Pd	$86.3 \pm 0.2$	$80.6 \pm 0.1$
11	$\text{Fe}_3\text{O}_4/1,6$ -hexanediamine/Rh	$88.9 \pm 0.3$	$87.3 \pm 0.4$
12	$\text{Fe}_3\text{O}_4/1,6$ -hexanediamine/Pt	$93.2 \pm 0.5$	$90.8 \pm 0.3$

<sup>a</sup>  $\alpha$ -pinene 2.7 g, n( $\alpha$ -pinene): n(metal active site)=130, H<sub>2</sub> 5 MPa,  $160^\circ\text{C}$ , 5 h. C: conversion of  $\alpha$ -pinene. S: selectivity towards *cis*-pinane. C and S determined by GC. Entries 2, 4, 7–12 the loading of metal nanoparticles was 10 wt%.

<sup>b</sup> Reused after five runs.

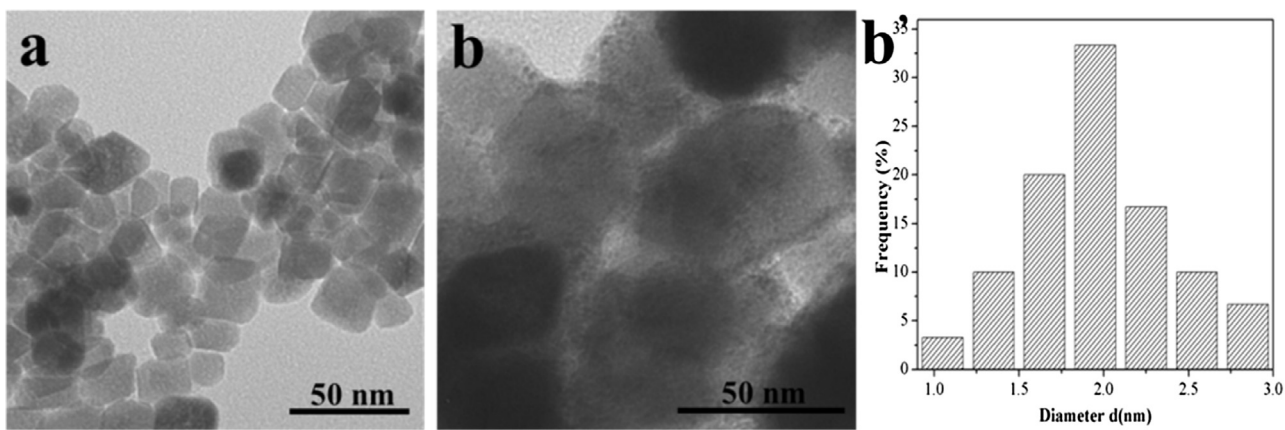


Fig. 2. TEM of  $\text{Fe}_3\text{O}_4/1$ , 6-hexanediamine (a), TEM and particle distributions of  $\text{Fe}_3\text{O}_4/1$ , 6-hexanediamine/Ru (b and b').

Table 2

Effect of different carbon chain length on the hydrogenation result.<sup>a</sup>

Entry	Catalyst	N/wt% <sup>b</sup>	Ru/wt% <sup>c</sup>	C/%	S/%
1	$\text{Fe}_3\text{O}_4/1$ , 2-ethylenediamine/Ru	3.12	5.95	$85.1 \pm 0.1$	$95.9 \pm 0.1$
2	$\text{Fe}_3\text{O}_4/1$ , 4-butanediamine/Ru	2.91	6.13	$93.6 \pm 0.2$	$96.8 \pm 0.2$
3	$\text{Fe}_3\text{O}_4/1$ , 6-hexanediamine/Ru	2.74	8.15	$99.2 \pm 0.3$	
4	$\text{Fe}_3\text{O}_4/1$ , 8-octanediamine/Ru	2.32	6.51	$95.1 \pm 0.1$	$96.7 \pm 0.1$
5	$\text{Fe}_3\text{O}_4/1$ , 12-dodecanediamine/Ru	2.08	5.94	$83.6 \pm 0.1$	$96.6 \pm 0.1$

<sup>a</sup>  $\alpha$ -pinene 2.7 g, catalyst ( $\text{Ru}$  10 wt%) 0.16 g,  $\text{H}_2$  5 MPa,  $160^\circ\text{C}$ , 5 h.

<sup>b</sup> N content determined by XPS.

<sup>c</sup> Ru content determined by ICP-AES. C: conversion of  $\alpha$ -pinene. S: selectivity towards *cis*-pinane. C and S determined by GC.

Ru nanoparticles were uniformly decorated on the  $\text{Fe}_3\text{O}_4/1$ , 6-hexanediamine and nearly all the Ru nanoparticles (particles size  $1.95 \pm 0.3$  nm) were connected with  $\text{Fe}_3\text{O}_4/1$ , 6-hexanediamine. As a result,  $\text{Fe}_3\text{O}_4/1$ , 6-hexanediamine/Ru made the catalytic active center Ru(0) highly dispersed and offered the reaction a large area interface, thus enhancing hydrogenation [38]. When Pd, Rh or Pt nanoparticles were loaded on the  $\text{Fe}_3\text{O}_4/1$ , 6-hexanediamine and used to catalyze the hydrogenation reaction, the results were not satisfying. This may be due to the fact that in the products obtained in the present work, the Ru nanoparticles with smaller average size ( $1.95 \pm 0.3$  nm) were evenly dispersed on the surface of  $\text{Fe}_3\text{O}_4/1$ , 6-hexanediamine (Fig. 2b and b') [39]. As shown in Fig. S4, the average diameter of Pd, Rh and Pt on the  $\text{Fe}_3\text{O}_4/1$ , 6-hexanediamine used here was about  $3.0 \pm 0.2$  nm.

### 3.2. Effects of different carbon chain length on the reaction

Different carbon chain length was used to prepare a series of amine-functionalized magnetite nanoparticles. Ru nanoparticles were loaded onto the obtained amine-functionalized magnetite nanoparticles with different carbon chain length and used to catalyze the hydrogenation reaction. The results are reported in Table 2. The used amine group content in the mixed solution was kept the same for the different carbon chain functionalized catalysts. XPS analyses showed that the amine group decreased upon increasing the length of carbon chain. This may be due to the fact that long-chain carbon molecules are relatively stable in the reaction and result in less amine groups modified in the  $\text{Fe}_3\text{O}_4$  nanoparticle [40]. As shown in Table 2, with the decrease of amine group that less amine groups served as anchors to immobilize Ru nanoparticles, the measured Ru content in the catalyst was reduced (Entries 3–5). This was attributed to less amine groups served as anchors to immobilize Ru nanoparticles. Interestingly, when the length of carbon chain less than six the measured Ru content was less than  $\text{Fe}_3\text{O}_4/1$ , 6-hexanediamine/Ru (Entries 1–3). This can be explained by the fact that when the length of carbon chain too

short, amine group cling to the surface of  $\text{Fe}_3\text{O}_4$ , a Ru nanoparticle will cover several amine group. The amine group will have a bigger space by increasing the length of carbon chain, which increases the Ru loading. Their properties upon the hydrogenation of  $\alpha$ -pinene were investigated. It was found that the conversion of  $\alpha$ -pinene increased with increasing the length of carbon chain when the length of carbon chain less than six (Entries 1–3). Upon increasing the length of carbon chain, the conversion of  $\alpha$ -pinene decreased. When the length of carbon chain was six, the hydrogenation of  $\alpha$ -pinene was effectively catalyzed.

### 3.3. Effects of different amounts of Ru nanoparticles on the reaction

$\text{Fe}_3\text{O}_4/1$ , 6-hexanediamine/Ru with various loading amounts of Ru nanoparticles was synthesized through a similar process as the one described earlier. The amount of Ru used during loading was 3 wt%, 6 wt%, 10 wt%, 13 wt% and 15 wt%. The Ru content in  $\text{Fe}_3\text{O}_4/1$ , 6-hexanediamine/Ru was determined by the ICP-AES technique and the results are reported in Table 3.  $\text{Fe}_3\text{O}_4/1$ , 6-hexanediamine/Ru with different amounts of Ru was used to catalyze the hydrogenation of  $\alpha$ -pinene (Table 3). It was found that

Table 3

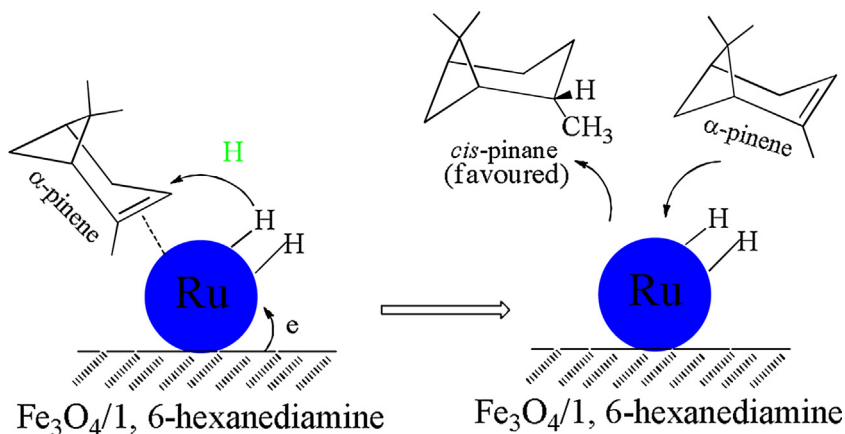
Effects of different amounts of Ru nanoparticles on the hydrogenation reaction.<sup>a</sup>

Entry	Ru/wt% <sup>b</sup>	Ru/wt% <sup>c</sup>	C/%	S/%
1	3	2.52	$78.6 \pm 1.5$	$95.1 \pm 0.6$
2	6	4.94	$85.1 \pm 0.4$	$96.3 \pm 0.3$
3	10	8.15	$99.2 \pm 0.3$	$97.1 \pm 0.2$
4	13	10.79	$99.3 \pm 0.2$	$97.2 \pm 0.1$
5	15	12.63	$99.2 \pm 0.2$	$97.1 \pm 0.1$

<sup>a</sup>  $\alpha$ -pinene 2.7 g,  $\text{Fe}_3\text{O}_4/1$ , 6-hexanediamine/Ru 0.16 g,  $\text{H}_2$  5 MPa,  $160^\circ\text{C}$ , 5 h. C: conversion of  $\alpha$ -pinene. S: selectivity towards *cis*-pinane.

<sup>b</sup> Ru content in the loading process.

<sup>c</sup> Ru content determined by ICP-AES in the  $\text{Fe}_3\text{O}_4/1$ , 6-hexanediamine/Ru. C and S determined by GC.



**Scheme 3.** The proposed mechanism of the hydrogenation of  $\alpha$ -pinene in the presence of  $\text{Fe}_3\text{O}_4/1$ , 6-hexanediamine/Ru.

the conversion of  $\alpha$ -pinene increased with increasing amounts of Ru. When the Ru nanoparticles content was 10%, the hydrogenation of  $\alpha$ -pinene was effectively catalyzed (Entry 3). This could be explained by the fact that with increasing Ru dosage,  $\text{Fe}_3\text{O}_4/1$ , 6-hexanediamine/Ru offers much more active sites enhancing hydrogenation [41]. A further increase in the Ru nanoparticle content above 10% brought no additional benefit to the hydrogenation reaction. This value was therefore selected as optimal.

Based on the above results, the mechanism of  $\alpha$ -pinene hydrogenation in the presence of  $\text{Fe}_3\text{O}_4/1$ , 6-hexanediamine/Ru was proposed and is shown in **Scheme 3**. In the initial stage,  $\alpha$ -pinene can be easily absorbed on the surface of the catalyst.  $\text{H}_2$  is activated by the electronically supported Ru. The bulky *gem*-dimethyl group inhibits absorption of the  $\beta$ -face of  $\alpha$ -pinene on the surface of the catalyst. Hydrogenation therefore takes place preferentially from the  $\alpha$ -face of the molecule, increasing thus selectivity towards *cis*-pinane [42].

### 3.4. The effects of the reaction conditions on the reaction results

**Fig. 3** shows the effects of the reaction conditions on the hydrogenation of  $\alpha$ -pinene. It was found that the conversion of  $\alpha$ -pinene increased upon increasing the dosage of catalyst. When the catalyst dosage was 4%, the conversion of  $\alpha$ -pinene was 98.6%. This was attributed to a high Ru dosage,  $\text{Fe}_3\text{O}_4/1$ , 6-hexanediamine/Ru offers much more active sites enhancing hydrogenation [43]. After that, no further increase in the reaction conversion of  $\alpha$ -pinene upon increasing the catalyst dosage could be obtained. With the enhancement of temperature, the conversion of  $\alpha$ -pinene dramatically increased, however, the selectivity for *cis*-pinane decreased. The reason might be that the higher temperature the more fierce of the electron shaking so the conversion of  $\alpha$ -pinene increased and reduced the selectivity of the reaction by increasing the number of accessible reaction pathways [44]. Therefore, 100 °C was the optimal reaction temperature. The effect of reaction time on

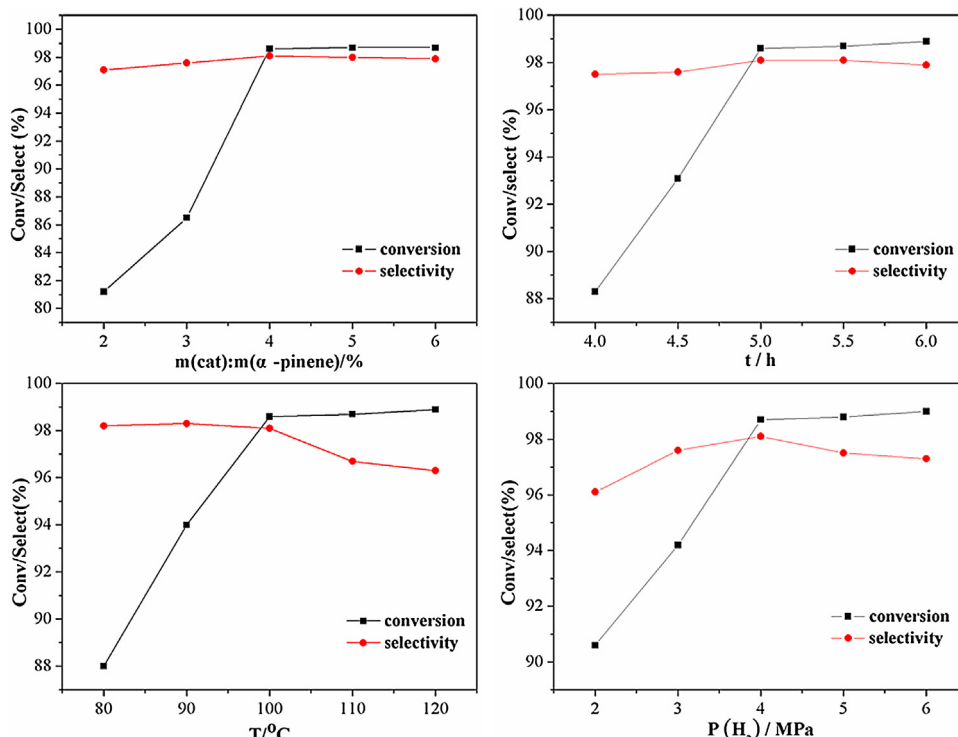


**Fig. 3.** The effects of the reaction conditions on the reaction results. Reaction conditions: catalyst:  $\text{Fe}_3\text{O}_4/1$ , 6-hexanediamine/Ru,  $P = 2.0\text{--}6.0 \text{ MPa}$ ,  $T = 80\text{--}120^\circ\text{C}$ ,  $t = 4.0\text{--}6.0 \text{ h}$ ,  $\alpha$ -pinene: 2.7 g,  $m(\text{catalyst}):m(\alpha\text{-pinene})\% = 2\text{--}6$ .

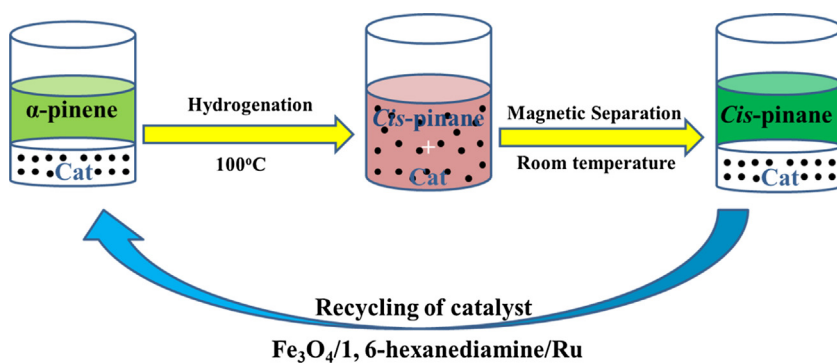


**Fig. 4.** Reaction scheme for the recycling of catalyst.

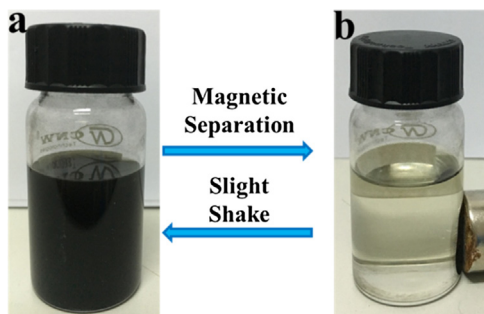


**Fig. 5.** Photograph of the catalyst dispersed in reaction mixture (a) and magnetic separation of the catalysts from the reaction medium (b).

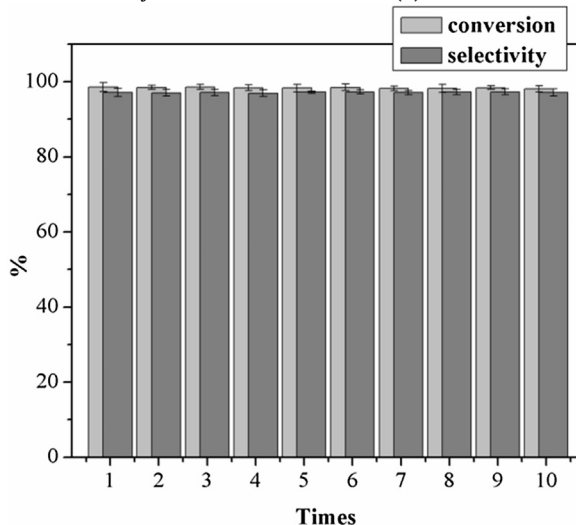


**Fig. 6.** The reusability of  $\text{Fe}_3\text{O}_4/1, 6\text{-hexanediamine/Ru}$ . Reaction conditions:  $\alpha$ -pinene 2.7 g,  $\text{Fe}_3\text{O}_4/1, 6\text{-hexanediamine/Ru}$  0.11 g (Ru 10 wt%),  $\text{H}_2$  4.0 MPa,  $100^\circ\text{C}$ , 5 h.

the reaction is also shown in Fig. 3. It was found that the conversion approximately trended to be stable when the reaction time exceeded 5.0 h. Therefore, the optimal reaction time was 5.0 h. The conversion increased with aggrandizing  $\text{H}_2$  pressure. However, the use of high pressure would increase the capital costs for the hydrogenation plant facility. Therefore, the optimal  $\text{H}_2$  pressure of 4.0 MPa was chosen. Based on the above results, the optimum reaction conditions were obtained as follows:  $P = 4.0 \text{ MPa}$ ,  $T = 100^\circ\text{C}$ ,  $t = 5.0 \text{ h}$ ,  $m(\text{catalyst}):m(\alpha\text{-pinene}) = 4\%$ . Under these conditions, the conversion of  $\alpha$ -pinene and the selectivity of *cis*-pinane were 98.6% and 98.1%, respectively.

### 3.5. The reusability of the catalyst

The recycling of the catalyst is shown in Fig. 4.  $\text{Fe}_3\text{O}_4/1, 6\text{-hexanediamine/Ru}$  was easily recovered by an external magnet when the reaction was finished, and dispersed quickly through a slight shake when the magnetic field was removed (Fig. 5). The recovered  $\text{Fe}_3\text{O}_4/1, 6\text{-hexanediamine/Ru}$  was directly used in the recycling experiments to investigate its reusability. Recycling experiments were conducted under the optimized reaction conditions and the results shown in Fig. 6. It was seen that the  $\text{Fe}_3\text{O}_4/1, 6\text{-hexanediamine/Ru}$  could be reused ten times without any obvious decrease in the reaction conversion and selectivity of the products under the given conditions. Therefore, the  $\text{Fe}_3\text{O}_4/1, 6\text{-hexanediamine/Ru}$  catalyst showed excellent reusable performance in the hydrogenation of  $\alpha$ -pinene. The good reusability of  $\text{Fe}_3\text{O}_4/1, 6\text{-hexanediamine/Ru}$  is attributed to the strong stability of  $\text{Fe}_3\text{O}_4/1, 6\text{-hexanediamine}$  to the Ru nanoparticles, which originates from the presence of multiple amines functional groups on the surface of  $\text{Fe}_3\text{O}_4/1, 6\text{-hexanediamine}$  and the very limited loss of the  $\text{Fe}_3\text{O}_4/1, 6\text{-hexanediamine/Ru}$  that were separated by applying an external magnetic field.  $\text{Fe}_3\text{O}_4/1, 6\text{-hexanediamine/Ru}$  own the higher saturated magnetization value ( $61.6 \text{ emu g}^{-1}$ ) and the superparamagnetic properties (Fig. S5). Fig. 7 showed the

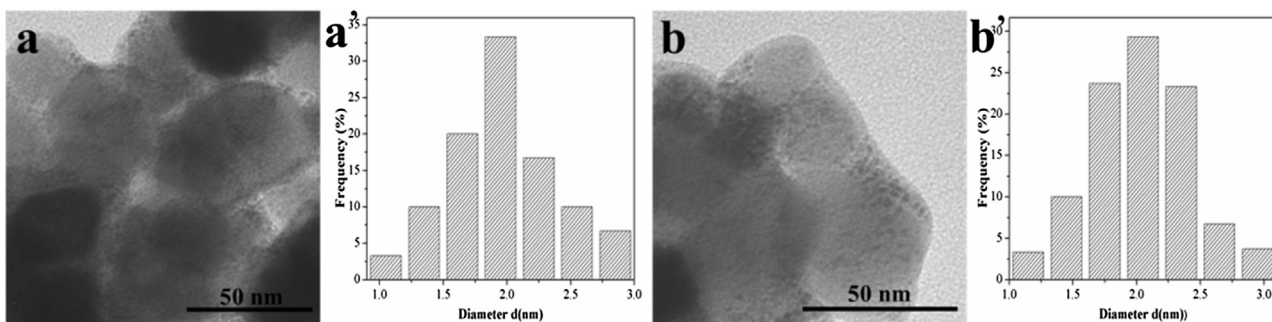


**Fig. 7.** TEM and particle distributions of unused  $\text{Fe}_3\text{O}_4/1, 6\text{-hexanediamine/Ru}$  (a and a') and repeatedly used  $\text{Fe}_3\text{O}_4/1, 6\text{-hexanediamine/Ru}$  for ten times (b and b').

TEM images of unused  $\text{Fe}_3\text{O}_4/1$ , 6-hexanediamine/Ru and the  $\text{Fe}_3\text{O}_4/1$ , 6-hexanediamine/Ru for ten repeatedly used. It was seen that numerous monodispersed nanoparticles were still uniformly dispersed on the  $\text{Fe}_3\text{O}_4/1$ , 6-hexanediamine after ten cycles. ICP-AES elemental analyses showed that the content of Ru and Fe was 8.13 wt% and 59.62 wt%, respectively. Its initial content was 8.15 wt% and 59.61 wt%. Nearly no appreciable Ru and Fe leaching into the organic phase were observed, as indicated by the ICP-AES analysis results of 0.79 and 2.36 ppm, respectively. All these results, indicate that the reusability of the  $\text{Fe}_3\text{O}_4/1$ , 6-hexanediamine/Ru catalyst is good.

#### 4. Conclusions

In summary, the magnetic  $\text{Fe}_3\text{O}_4/1$ , 6-hexanediamine/Ru catalyst, consisting of Ru nanoparticles supported on amine-functionalized magnetite nanoparticles were synthesized and successfully applied to the hydrogenation reaction of  $\alpha$ -pinene to form *cis*-pinane.  $\text{Fe}_3\text{O}_4/1$ , 6-hexanediamine/Ru had good superparamagnetic properties and that the introduction of the amine-functionalized improved the monodispersity, morphological regularity and size uniformity of the Ru nanoparticles.  $\text{Fe}_3\text{O}_4/1$ , 6-hexanediamine/Ru exhibited an outstanding catalytic performance with 98.6% conversion and 98.1% selectivity for *cis*-pinane.  $\text{Fe}_3\text{O}_4/1$ , 6-hexanediamine/Ru was easily separated from the product by applying an external magnetic field and  $\text{Fe}_3\text{O}_4/1$ , 6-hexanediamine had a strong stability towards Ru nanoparticles, originating from the numerous amines functional groups on the surface of  $\text{Fe}_3\text{O}_4/1$ , 6-hexanediamine. Both factors made  $\text{Fe}_3\text{O}_4/1$ , 6-hexanediamine/Ru exhibit good reusability.

#### Acknowledgements

This work was financially supported by the Taishan Scholar Program of Shandong, the National Natural Science Foundation of China (31270615). The authors are grateful for the financial support.

#### Appendix A. Supplementary data

Supplementary data associated with this article can be found, in the online version, at <http://dx.doi.org/10.1016/j.molcata.2016.09.007>.

#### References

- [1] Y. Yang, X. Liu, D. Yin, Z. Zhang, D. Lei, J. Yang, *J. Ind. Eng. Chem.* 26 (2015) 333–334.
- [2] I.L. Simakova, Y. Solkina, I. Deliy, J. Wärnå, D.Y. Murzin, *Appl. Catal. A: Gen.* 356 (2009) 216–224.
- [3] L. Wang, H. Guo, X. Chen, Q. Chen, X. Wei, Y. Ding, B. Zhu, *Catal. Sci. Technol.* 5 (2015) 3340–3351.
- [4] M. Sudhakar, V.V. Kumar, G. Naresh, M.L. Kantam, S. Bhargava, A. Venugopal, *Appl. Catal. B: Environ.* 180 (2016) 113–120.
- [5] H. Wan, A. Vitter, R.V. Chaudhari, B. Subramaniam, *J. Catal.* 309 (2014) 174–184.
- [6] M.P. Boone, D.W. Stephan, *J. Am. Chem. Soc.* 135 (2013) 8508–8511.
- [7] M.G. Al-Shaal, A. Dzierbinski, R. Palkovits, *Green Chem.* 16 (2014) 1358–1364.
- [8] X. Yang, S. Liu, C. Xie, S. Yu, F. Liu, *Chin. J. Catal.* 32 (2011) 643–646.
- [9] S. Hou, C. Xie, H. Zhong, S. Yu, *RSC Adv.* 5 (2015) 89552–89558.
- [10] R.N. Baig, R.S. Varma, *ACS Sustain. Chem. Eng.* 2 (2014) 2155–2158.
- [11] B. Kaboudin, R. Mostafalu, T. Yokomatsu, *Green Chem.* 15 (2013) 2266–2274.
- [12] M. Shao, F. Ning, J. Zhao, M. Wei, D.G. Evans, X. Duan, *J. Am. Chem. Soc.* 134 (2012) 1071–1077.
- [13] Y. Wang, L. Zhang, X. Gao, L. Mao, Y. Hu, X.W.D. Lou, *Small* 10 (2014) 2815–2819.
- [14] M. Shokouhimehr, K.Y. Shin, J.S. Lee, M.J. Hackett, S.W. Jun, M.H. Oh, J. Jang, T. Hyeon, *J. Mater. Chem. A* 2 (2014) 7593–7599.
- [15] M. Shokouhimehr, *Catalysts* 5 (2015) 534–560.
- [16] S.W. Jun, M. Shokouhimehr, D.J. Lee, Y. Jang, J. Park, T. Hyeon, *Chem. Commun.* 49 (2013) 7821–7823.
- [17] R.S. Mahdi, K. Aeung, S. Mohammadreza, *Nanosci. Nanotechnol. Lett.* 6 (2014) 309–313.
- [18] K.H. Choi, M. Shokouhimehr, Y.E. Sung, *Bull. Korean Chem. Soc.* 34 (2013) 1477–1480.
- [19] Z. Zhang, H. Duan, S. Li, Y. Lin, *Langmuir* 26 (2010) 6676–6680.
- [20] Y. Du, W. Liu, R. Qiang, Y. Wang, X. Han, J. Ma, P. Xu, *ACS Appl. Mater. Interfaces* 6 (2014) 12997–13006.
- [21] C. Ma, C. Li, N. He, F. Wang, N. Ma, L. Zhang, Z. Lu, Z. Ali, Z. Xi, X. Li, *J. Biomed. Nanotechnol.* 8 (2012) 1000–1005.
- [22] S. Pan, Y. Zhang, H. Shen, M. Hu, *Chem. Eng. J.* 210 (2012) 564–574.
- [23] F. Zhang, J. Jin, X. Zhong, S. Li, J. Niu, R. Li, J. Ma, *Green Chem.* 13 (2011) 1238–1243.
- [24] Y. Deng, Y. Cai, Z. Sun, J. Liu, C. Liu, J. Wei, W. Li, C. Liu, Y. Wang, D. Zhao, *J. Am. Chem. Soc.* 132 (2010) 8466–8473.
- [25] M.J. Jin, D.H. Lee, *Angew. Chem. Int. Ed.* 49 (2010) 1119–1122.
- [26] P. Wang, H. Zhu, M. Liu, J. Niu, B. Yuan, R. Li, J. Ma, *RSC Adv.* 4 (2014) 28922–28927.
- [27] F. Zhang, N. Liu, P. Zhao, J. Sun, P. Wang, W. Ding, J. Liu, J. Jin, J. Ma, *Appl. Surf. Sci.* 263 (2012) 471–475.
- [28] A. Khalafi-Nezhad, F. Panahi, *ACS Sustain. Chem. Eng.* 2 (2014) 1177–1186.
- [29] M. Ma, Q. Zhang, D. Yin, J. Dou, H. Zhang, H. Xu, *Catal. Commun.* 17 (2012) 168–172.
- [30] J. Wang, B. Xu, H. Sun, G. Song, *Tetrahedron Lett.* 54 (2013) 238–241.
- [31] P. Wang, F. Zhang, Y. Long, M. Xie, R. Li, J. Ma, *Catal. Sci. Technol.* 3 (2013) 1618–1624.
- [32] A. Sandoval, C. Louis, R. Zanella, *Appl. Catal. B: Environ.* 140 (2013) 363–377.
- [33] B.T. Loveless, C. Buda, M. Neurock, E. Iglesia, *J. Am. Chem. Soc.* 135 (2013) 6107–6121.
- [34] J. Mitra, X. Zhou, T. Rauchfuss, *Green Chem.* 17 (2015) 307–313.
- [35] L. Shang, T. Bian, B. Zhang, D. Zhang, L.Z. Wu, C.H. Tung, Y. Yin, T. Zhang, *Angew. Chem. Int. Ed.* 53 (2014) 250–254.
- [36] H. Kirsch, X. Zhao, Z. Ren, S.V. Levchenko, M. Wolf, R.K. Campen, *J. Catal.* 320 (2014) 89–96.
- [37] Y.-R. Hu, C. Guo, F. Wang, S.-K. Wang, F. Pan, C.-Z. Liu, *Chem. Eng. J.* 242 (2014) 341–347.
- [38] H. Xu, S. Ouyang, P. Li, T. Kako, J. Ye, *ACS Appl. Mater. Interfaces* 5 (2013) 1348–1354.
- [39] H. Wei, C. Gomez, J. Liu, N. Guo, T. Wu, R. Lobo-Lapidus, C.L. Marshall, J.T. Miller, R.J. Meyer, *J. Catal.* 298 (2013) 18–26.
- [40] Q. Yan, F. Yu, J. Liu, J. Street, J. Gao, Z. Cai, J. Zhang, *Bioresour. Technol.* 127 (2013) 281–290.
- [41] A. Verdaguera-Casadevall, D. Deiana, M. Karamad, S. Siahrostami, P. Malacrida, T.W. Hansen, J. Rossmeisl, I. Chorkendorff, I.E. Stephens, *Nano Lett.* 14 (2014) 1603–1608.
- [42] W. Cocker, P.V.R. Shannon, P.A. Staniland, *J. Chem. Soc. C* 1 (1966) 41–47.
- [43] H. Zhang, Y. Lei, A.J. Kropf, G. Zhang, J.W. Elam, J.T. Miller, F. Sollberger, F. Ribeiro, M.C. Akatay, E.A. Stach, *J. Catal.* 317 (2014) 284–292.
- [44] S.-H. Ko, T.-C. Chou, T.-J. Yang, *Ind. Eng. Chem. Res.* 34 (1995) 457–467.